



## Hydraulic Calculations of a Slotted Separator Using the SSIIM Program

*Paweł Zawadzki\**

*Poznan University of Life Sciences, Poland  
<https://orcid.org/0000-0002-5425-4669>*

*Zbigniew Walczak*

*Poznan University of Life Sciences, Poland  
<https://orcid.org/0000-0003-3999-7250>*

*Jakub Nieć*

*Poznan University of Life Sciences, Poland  
<https://orcid.org/0000-0002-9864-057X>*

*Mateusz Hämmerling*

*Poznan University of Life Sciences, Poland  
<https://orcid.org/0000-0001-9093-4365>*

*\*corresponding author's e-mail: [pawel.zawadzki@up.poznan.pl](mailto:pawel.zawadzki@up.poznan.pl)*

**Abstract:** Analysis of the results of the hydraulic calculations of a slotted separator allowed for changes in the separator design, considering the reduction of flow turbulence, ensuring the continuity of water flow and sediments, and the optimal location of the slots. The separator is a crucial element of the installation for the hydromechanical removal of sediments from the bottom of a water reservoir. Tests were carried out on the physical and mathematical models. Hydraulic calculations and numerical simulations were carried out using the SSIIM (Simulation of sediment movements in water intakes with multiblock option) program. The program enables three-dimensional analysis of flows and transport of sediments in rivers and canals by solving the Navier-Stokes equation and the turbulent model  $k-\epsilon$ . In addition, several numerical experiments of the separator work were carried out for various design solutions regarding the geometry of the inlet and outlet channels and their connection with the chambers and slots system. Finally, the numerical simulations and conducted research on a physical model allowed us to develop an optimal solution.

**Keywords:** water reservoir, sediment removal, slotted separator, SSIIM



## 1. Introduction

The construction and operation of reservoirs or other damming structures on rivers are related to the interruption of water flow and water sediment transport by water. This contributes to two unfavourable phenomena:

- retaining/deposited sediment transported by water flow in the reservoir and reducing its usable capacity,
- the erosion of a bed and banks of the river channel below the damming.

So far, the solutions focus primarily on separately preventing the effects of erosion below the damming structure or removing sediments from the reservoir.

The most appropriate solution seems to be to create conditions for the continuous flow of sediments from the upper to the lower stand of the damming structure. The installation for hydromechanical removal of sediments from the bottom of the reservoir, designed by Zawadzki & Błażejowski (2018), allows their transport with simultaneous sorting into two streams: thicker mineral sediments are directed directly to the river, fine mineral and organic fractions can be utilised (for example in agriculture or forestry). The sediment removal and separation installation use only the difference in water levels between the upper and lower stands of the damming structure.

The main element of the Zawadzki & Błażejowski (2018) installations is the slotted separator (Fig. 1), which, under appropriate hydraulic conditions (volumetric flow rate, average velocities), enables the transport and separation of removed sludge. However, moving all sediment (without separation) below the damming structure may contribute to the deterioration of river water quality.

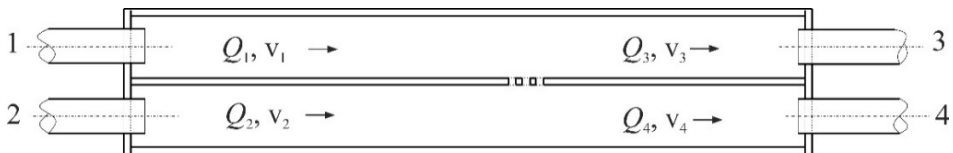


**Fig. 1.** Slotted separator longitudinal section: 1 – water inlet with being removed sediments, 2 – clean water inlet, 3 – the outflow of water and fine (undesirable) fractions, 4 – outflow of water and coarse (desirable) mineral fractions

Brandt (1999) draws attention to the deterioration of water quality below the damming, especially during the reservoir flushing period. Among the adverse effects, the author mentions, among others: a decrease in the pH of water, an increase in the concentration of phosphorus and nitrogen compounds, a significant increase in the content of organic matter in sediments, and a decrease in the amount of oxygen dissolved in water. Water quality can reach levels that

threaten organisms below the reservoir. Brandt (1999) also finds a significant relationship between sediment grain size and organic matter content, which is more prominent for smaller grains. Studies by Madeyski et al. (2008) confirm the absorption capacity of heavy metals by organic parts contained in bottom sediments, but they do not find a significant relationship between bottom grain size sediment (a content of fine fractions) and the content of heavy metals.

Therefore, it seems appropriate to sort out fine fractions from the removed sediments and subject them to further utilisation. Thicker mineral fractions, without risk of deterioration of water quality, can be directed to the river. Their presence in the watercourse below the horizontal apron should limit the local erosion of the river bed and banks. This method of “feeding the sediment” of the river seems to be less technical than the measures taken, for example, at the Iffezheim on the Rhine, consisting in overwhelming a scour hole with sediments extracted in an inlet part of the reservoir (Parzonka et al. 2010, Hildebrant et al. 2017).

## 2. Slotted Separator Research's

### 2.1. Research on the Physical Model

In the first stage of research, simulations of the separator work on a physical model were carried out in the water laboratory of the Department of Water and Sanitary Engineering of the Poznan University of Life Sciences. The separator (Fig. 1) was made as a rectangular box with external dimensions: length 1020 mm, height 210 mm and width 100 mm. In the middle of the cuboid, height guides have been made to install a partition with slots and divide the separator into two working chambers with square cross-sections and dimensions of 80 x 80 mm. The cuboid was closed with front and rear panels, in which two holes with a diameter of 50 mm were made, allowing for feeding and draining of the mixtures from the upper and lower separator duct. In the tests, the removed and separated sediment was simulated using spherical particles with a diameter of 6.0 mm, made of materials with a density from 1000-2650 kg·m<sup>-3</sup> (Zawadzki et al. 2018).

Two series of experiments **A** and **B** were carried out, using a mixture composed of two fractions of different densities (bidepressive mixture) to create and determine the conditions of hydraulic sorting easily. In both series, tests were carried out at four water flow velocities (0.4 m·s<sup>-1</sup>, 0.45 m·s<sup>-1</sup>, 0.5 m·s<sup>-1</sup> and 0.55 m·s<sup>-1</sup>; measurements in the separator above the slots) and were repeated at a different total weight of dosed solid particles (feed: 400 g, 600 g and 1000 g, respectively). Studies have shown that it is possible to create such hydraulic conditions where the separation of sludge into two fractions occurs and their further transport by two lines. It allows the separation of thicker mineral fractions (gravel, coarse and medium sand) from organic impurities and finer min-

eral fractions in the form of a suspension. The relationship between the flow speed of the mixture above the slots and the velocity of falling of grains turned out to be significant (Zawadzki et al. 2018). Laboratory tests have also shown various design flaws of the slotted separator: rapid changes in cross-section affecting the turbulence of the flow, which hindered the separation, and edges/thresholds at which the transported material accumulated. Mathematical simulations were conducted to improve the constructions of the slotted separator.

## 2.2. Simulation of Separator Using the Mathematical Model

The results of tests on the physical model only partly met the expectations related to the work of the slotted separator. These indicated further directions for separator testing:

- changes in the construction of the separator's working chamber in order to smoothly feed the hydro-mixture into the slots,
- determining the number and size of slots and their impact on sorting efficiency,
- determination of optimal hydraulic conditions for the separation of specific sediment diameters.

In the first stage of the research, the simulations of the slotted separator on a mathematical model were carried out under the clear water conditions flow. The purpose of this research was to generate a mathematical model mesh. The numerical separator was identical to that used in the physical model and then gradually introduced such changes to improve the water flow conditions through the separator in three areas: inlet to the separator's working chamber, slots, and outlet from the working chambers. It was assumed that the surfaces on which the hydro-mixture would be transported would be without thresholds, faults or unevenness, and the changes (expansion and narrowing) of the cross-section are to be gentle so as not to cause the water jets to detach from the flowing surface.

In water engineering, numerical methods are more common, both in designing seepage in earth dams and predicting clogging geotextile drainage (Niec et al. 2019). The numerical simulations of the slotted separator could be performed in the SSIIM software (Simulation of Sediment movements in water intakes with multiblock option). N.R.B. Olsen from the Norwegian University of Science and Technology in Trondheim developed the computer code (Olsen 2007, Olsen 2009). It was created for modelling sediment transport in rivers, reservoirs and below hydraulic structures. Olsen (2009) considered the main advantage of the SSIIM program to model sediment transport in troughs with a moving bottom with complex geometry. The program was used in calculations of water, and sediment flows through the sedimentation reservoir (Agrawal 2005, Singh et al. 2007), local erosion at the pillars (Abouzeid et al.

2006) and below the overflow (Hämmerling et al. 2013), as well as accumulation of sediments in the retention reservoir (Zhang et al. 2013) or erosion below it (Zhang et al. 2016).

### 2.3. Description of the mathematical model

In the SSIIM program, the three-dimensional, turbulent flow of a viscous, incompressible liquid is modelled by Navier-Stokes equations containing continuity equations (1) and momentum conservation equations (2), which after averaging over speed and pressure can be written as Reynolds equations (RANS) (Rüther 2006, Olsen 2014):

$$\frac{dU_i}{dx_i} = 0 \quad (i=1,2,3) \quad (1)$$

$$\frac{\partial U_i}{\partial t} + U_j \frac{\partial U_i}{\partial x_j} = \frac{1}{\rho} \frac{\partial}{\partial x_j} \left( -P \delta_{ij} - \overline{\rho u'_i u'_j} \right) \quad (i, j = 1, 2, 3) \quad (2)$$

where:

$U_i$  – velocity averaged over time  $x_i$ ,

$t$  – time,

$\rho$  – water density,

$P$  – pressure,

$\delta_{ij}$  – Kronecker delta, which takes the value 1 when  $i=j$ , and in other cases, it is equal to 0,

$x_i x_j$  – coordinates in the tensor notation,

$\overline{\rho u'_i u'_j}$  – Reynolds stress ( $u'$  – pulsation velocity).

The relationship proposed by Boussinesq describes Reynolds stresses:

$$\overline{u'_i u'_j} = \nu \left( \frac{\partial U_j}{\partial x_i} + \frac{\partial U_i}{\partial x_j} \right) - \frac{2}{3} k \delta_{ij} \quad (3)$$

where:

$\nu$  – turbulent viscosity coefficient (turbulent exchange, vortex viscosity).

The  $k$ - $\varepsilon$  turbulence model allows to determine the turbulent viscosity coefficient from the relationship:

$$\nu = C_\mu \frac{k^2}{\varepsilon} \quad (4)$$

where:

$C_\mu = 0.09$  constant,

$k$  – turbulent kinetic energy defined as  $k = \frac{1}{2} \overline{u'_i u'_j}$ ,

$\varepsilon$  – energy dissipation velocity.

Turbulent kinetic energy can be modelled as follows:

$$\frac{\partial k}{\partial t} + U_j \left( \frac{\partial k}{\partial x_j} \right) = \frac{\partial}{\partial_j} \left( \frac{\nu}{\sigma_k} \frac{\partial k}{\partial x_j} \right) + P_k - \varepsilon \quad (5)$$

where:

$\sigma_k = 1.0$  and

$$P_k = \nu \frac{\partial U_j}{\partial x_i} \left( \frac{\partial U_j}{\partial x_i} + \frac{\partial U_i}{\partial x_j} \right) \quad (6)$$

However, the dissipation of kinetic energy  $\varepsilon$  is determined by the relationship:

$$\frac{\partial \varepsilon}{\partial t} + U_j \frac{\partial \varepsilon}{\partial x_j} = \frac{\partial}{\partial x_j} \left( \frac{\nu}{\sigma_\varepsilon} \frac{\partial \varepsilon}{\partial x_j} \right) + C_{\varepsilon 1} \frac{\varepsilon}{k} P_k - C_{\varepsilon 2} \frac{\varepsilon^2}{k} \quad (7)$$

where:

$\sigma_\varepsilon = 1.3$ ,  $C_{\varepsilon 1} = 1.44$  i  $C_{\varepsilon 2} = 1.92$ .

In equations (4)-(7)  $C_\mu$ ,  $\sigma_k$ ,  $\sigma_\varepsilon$ ,  $C_{\varepsilon 1}$  and  $C_{\varepsilon 2}$  are experimentally determined constants, and their values in the SSIIM computer code were adopted after Launder & Spalding (1974), Rodi (1980) and Olsen (2014).

Differential equations describing the water flow were solved numerically using the finite volume method (FVM), using the SIMPLE algorithm, which involves calculating iteratively alternating velocity and pressure components. Using the standard  $k$ - $\varepsilon$  model in RANS calculations introduces two additional equations determining Reynolds stresses to obtain a closed system of equations (Błóński 2009).

## 2.4. Assumptions, Simplifications Adopted

In the first simulations, the mathematical model of the separator relatively faithfully reproduced the physical model tested in the laboratory. The dimensions of the mathematical separator model were adopted following the dimensions of the physical model. The space occupied by water was discretised (length of the separator's working chamber  $L_k = 1.0$  m, width  $D_{rk} = 0.08$  m; the height of one chamber  $H_k = 0.09$  m), two 1.0 m long supply lines and 0.5 m long discharge lines (Fig. 2). It was assumed that with such a length of pipes, the boundary conditions would not affect the velocity distribution in the separator. It was also assumed that these wires would have a square cross-section of  $0.05 \times 0.05$  m. Considering the above values, the external dimensions of the modelled area (working chamber) were: length 2.5 m, height 0.19 m and width 0.08 m.

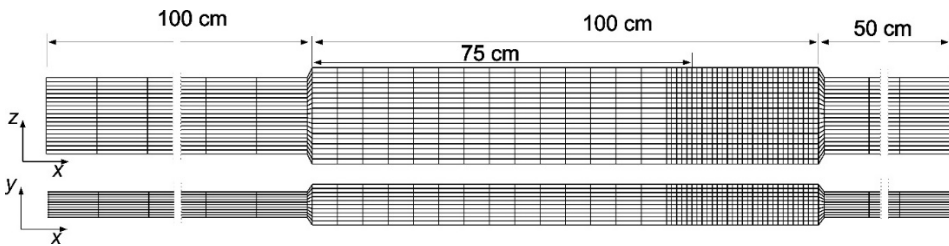


**Fig. 2.** Initial mesh version of the mathematical model of the slotted separator: longitudinal section and top view

The model mesh (discretisation of the calculation area) was modified during the simulation. The changes were related to, among others, the definition of slots and disturbances in the flow velocity vector field in cross-sections of expansion and narrowing. When creating the model's grid, the author's suggestions of SSIIM software were taken into account that the smallest flow area (gap) be created by at least two cells (Olsen 2009, Olsen 2014). The initial version adopted:

- vertical cross-sections ( $\Delta x$ ): in inlet and outlet pipes every 100 mm, in separator chambers every 50 mm, above and below the separator slots every 10 mm,
- longitudinal sections ( $\Delta y$ ): in pipes every 5 mm, in chambers every 8 mm,
- horizontal cross-sections ( $\Delta z$ ): in pipes every 8 mm, in chambers every 10 mm.

The change of the cross-section from the cross-section of the pipes leading to the cross-sections of the working chamber took place over a distance of 1 cm.

In the original version, flow through three 2 cm wide slots with a 2 cm gap was simulated. The first slot was located at  $\frac{3}{4}$  (75 cm) of the length of the work-

ing chamber (Fig. 3). The spaces between pipes (water inlet and outlet) and the space between the upper and lower working chamber were excluded from the flow (cells of the mathematical model are marked in grey).

The flow of solid particles and water between the upper and lower chamber of the separator was possible only through the slots (holes) generated in the partition separating both chambers. Initially, three mesh variants were adopted, in which the width of the slot in the longitudinal section was modelled by: two (variant: c2), four (c4) and six cells (c6) (Fig. 4). The mesh variants were analysed based on a vector image of the velocity field at a set flow of clean water.

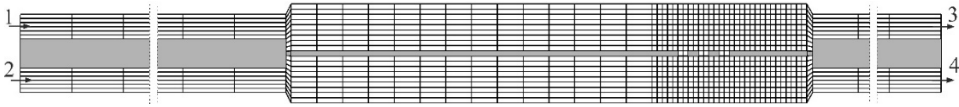


**Fig. 3.** Mathematical model mesh: gray area showing the area excluded from flow

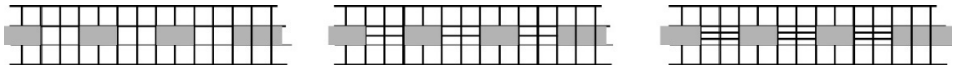


**Fig. 4.** Mathematical model grid in which 2 cm wide slots are modelled by 2, 4 and 6 cells

Taking into account the author of the SSIIM software (OLSEN 2014) recommendations for making the first calculations without using sediments and analysing the vector velocity field for compliance of the obtained flow image with reality. This analysis was performed for sensitive areas of the separator: expansion and narrowing at the connection of the separator with the pipes and water flow through the slots.

Simulations were carried out under the following conditions:

- a) equal volumetric water flow rates in all pipes  $Q_1 = Q_2 = Q_3 = Q_4 = 0.005 \text{ m}^3 \cdot \text{s}^{-1}$  (**simulation A**),
- b) at the flow inlet of  $Q_1 = 0.0055 \text{ m}^3 \cdot \text{s}^{-1}$   $Q_2 = 0.0045 \text{ m}^3 \cdot \text{s}^{-1}$ , at the flow outlet of  $Q_3 = Q_4 = 0.005 \text{ m}^3 \cdot \text{s}^{-1}$  (**simulation B**, forced flow through the slots).

The impact of inlet and outlet geometry on the transport and separation of individual sediment fractions was also analysed in detail.

## 2.5. Inlet Section

With an equal supply of both supply pipes (**simulation A**;  $Q_1 = Q_2 = Q_3 = Q_4$ ), the velocity vectors were similar in the variants c2, c4 and c6 (Figs. 5 and 6). This simulation shows significant flow disturbances at the inflow and outflow from the working chamber (rapid changes in cross-section). At the inlet to the upper working chamber (stream 1), the water stream breaks away from the bot-

tom of the supply pipe, resulting in a vortex with a horizontal axis of rotation reaching half the length of the working chamber (approx. 50 cm). The water flow directions at the bottom of the working chambers are opposite to the main-stream.

In the physical model studies, similar flow disturbances were observed, which caused:

- retaining some solid particles in the vortex;
- raising solid particles upwards and carried above the bottom of the working chamber.

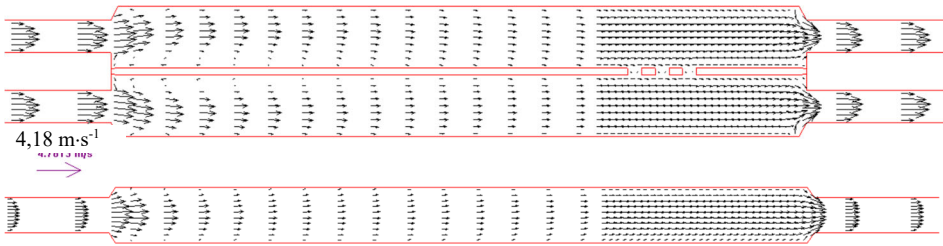


**Fig. 5.** Vector velocity field simulating the flow of  $5 \text{ dm}^3 \cdot \text{s}^{-1}$  (simulation A) through the slotted separator: at the top – longitudinal profile in the model axis, at the bottom – horizontal view of the inlet of the upper working chamber

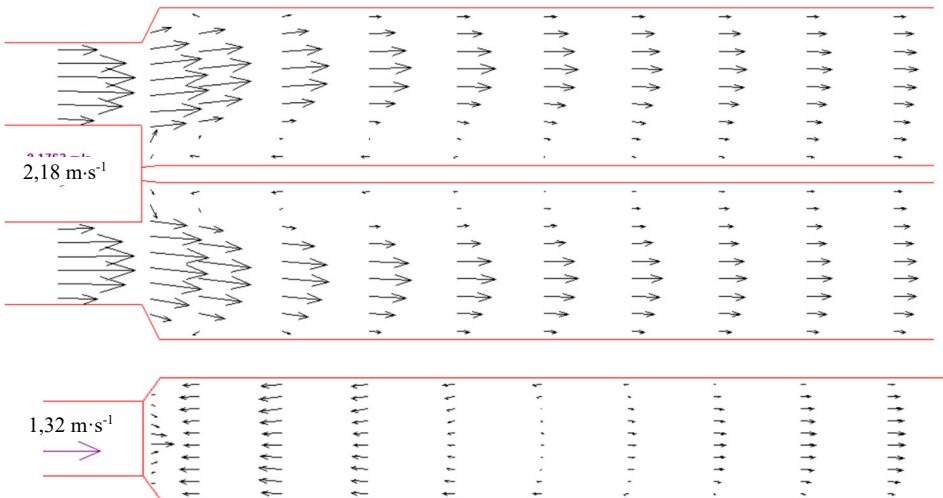


**Fig. 6.** Vector velocity field (simulation A) near the section connection pipes and separator: top – longitudinal profile in the model axis, at the bottom – horizontal view below the bottom of the guide pipe

These phenomena adversely affected the separator's efficiency because some solid particles' flow regimes changed from bedload to suspension. For the correct operation of the separator, creating and maintaining conditions for heterogeneous flow or, optionally, flow with a moving bed is more advantageous. These flows are characterised by the fact that the highest concentration of solid particles is at the bottom of the pipe and decreases in the upward direction. Assuming that partial sedimentation has already occurred in the water and solids feed pipe, the increased turbulence at the beginning of the separator's upper working chamber was very adverse.

Increasing the active cross-section of the separator chamber relative to the pipe cross-section reduces the average velocity and initiates the sedimentation of solid particles, but this should be done gently without increasing the turbulence of the stream. Therefore, two changes were proposed (Fig. 7): bringing the two pipes closer together so that there is no difference in the level of the bottom of the upper pipe and the separator chamber and a milder extension of the cross-section (introduction of a 10 cm diffuser in front of the working chamber).

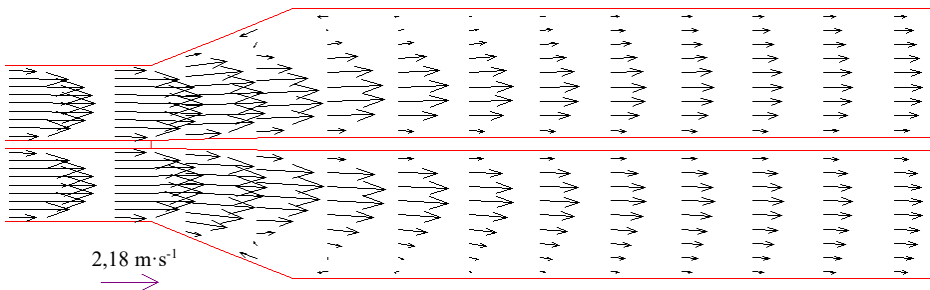


**Fig. 7.** Vector velocity field (A simulation) with a diffuser for pipes and separator connection; longitudinal profile in the model axis

Described changes allowed water with solids to flow into the upper working chamber without additional turbulence. The bedload was not picked up from the bottom and transferred downstream into the working chamber. Velocities opposite the main direction of flow occurred only in a limited area of the working chambers and did not affect the transported solid particles.

## 2.6. Outlet Section

The outflow of water and sorted sludge occurred via both pipes: lower fractions desirable, upper undesirable (polluting). Therefore, it is necessary to ensure the flow of both streams without obstacles. During presented tests on the physical model, difficulties in the flow of solid particles were observed when separator

was connected with chambers and pipes. It is also confirmed by numerical analyses for models S1 and S2 (Fig. 8). To avoid the above, the mathematical model proposes (model S3, Fig. 8):

- connection of the bottom of the pipes and the chamber on one level (without edges),
- lowering the outlet pipes,
- slight cross-section narrowing by introducing a 10 cm long confessor (2 diameters of the discharge pipes).

Introducing these changes eliminated the disturbance of the outflow velocities and should ensure a continuous flow of water and transported solids (Fig. 8).

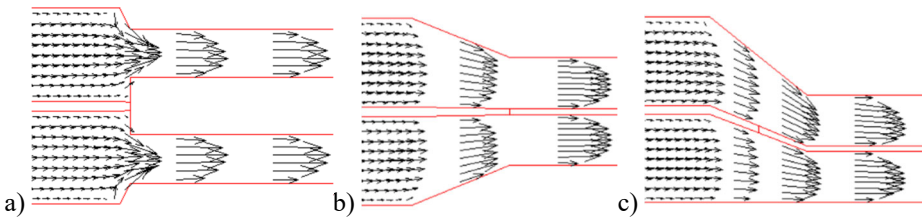


**Fig. 8.** Changes in the velocity vector field (A simulation) on the connection of separator and draining channels; longitudinal profile in the model axis; a) S1, b) S2, c) S3

The conducted simulations allowed the design and dimensioning of a new construction of the slotted separator presented in Fig. 9.

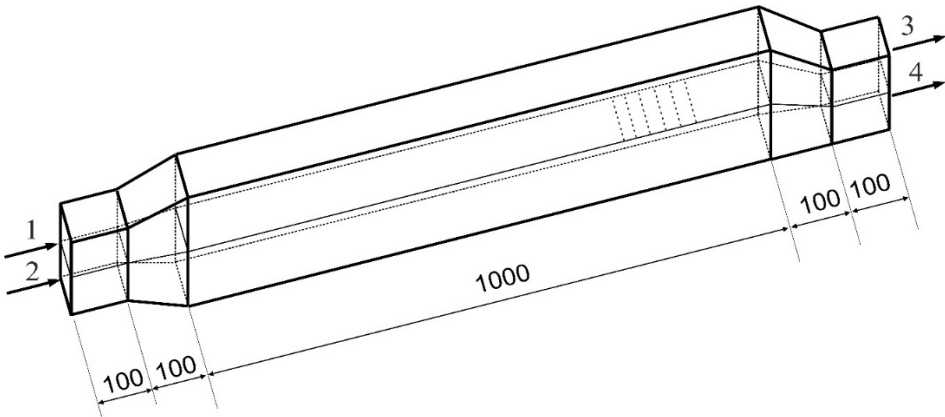


**Fig. 9.** Developed, optimal for hydraulic reasons geometry of the slotted separator (dimensions in mm)

## 2.7. Slots of Separator

Firstly, the impact of mesh discretisation in the vicinity of separator slots on the obtained results was analysed. Flow parameters are calculated for each cell in the finite volume method (FVM). Therefore, by increasing the number of cells forming the separator gap, a better quantitative and qualitative description of the velocity distribution can be expected. Next, modelling the work of separator slots was carried out under conditions of forced water flow through the slots (**B simulation**). In these simulations, the cumulative flow was forced  $Q_1 + Q_2 = 0.01 \text{ m}^3 \cdot \text{s}^{-1}$ . All variants (c2, c4, c6; Figs. 4 and 10) show uneven water flow in the initial and final part of the slot. Obviously, for the c6 scheme, in which the slots are modelled with 6 cells, a more detailed velocity distribution was obtained, but with two cells, the description is sufficiently accurate. Flow disorders are caused by the impact of water on the perpendicular wall of the partition closing the slot.

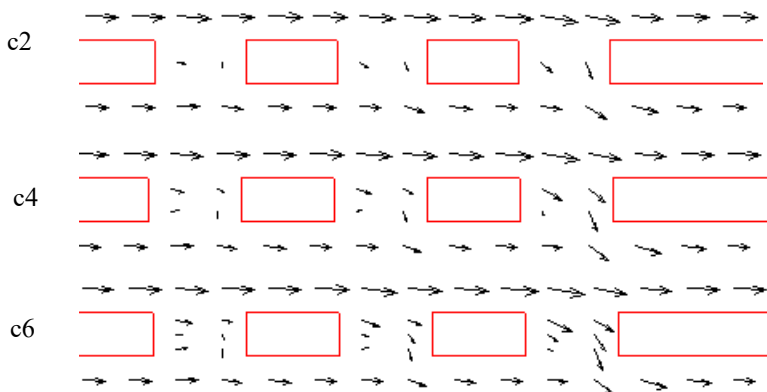


**Fig. 10.** Vector velocity field in slot simulations: mesh c2, c4 and c6

The discretisation of the modelled area in which the slot is described by more than 2 cells allows simulations of oblique cell work (Fig. 11).

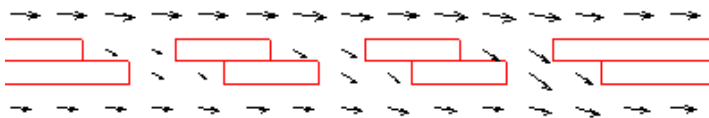


**Fig. 11.** Vector velocity field in the simulation of water flow through the system of oblique slots defined by 4 cells (c4) for each slot slanting

The flow of water through the oblique slots seems less chaotic. The velocity vectors are parallel to each other. It is also characteristic that the highest velocities were observed in the third and last slot. The use of an oblique slot requires its expansion (larger opening width both in simulations and in tests on a physical model), because the upper and lower edges of the slot approach each other, leaving a small space.

## 2.8. Velocity distribution in working chambers

In the beginning, the velocity distribution was analysed only in the longitudinal profile of the separator. However, it also seems important to analyse the velocity distributions in cross sections in the working chambers, especially in the upper chamber before the slots. In the simulations presented, horizontal cross-sections were distributed evenly every 1 cm at the height of the modelled area. However, the generation of mesh with a more significant number of cells (c4, c6) on the model requires adequate horizontal compaction of the grid, both within the slots as well as throughout the entire section of the section under consideration. In the final version of the S4 mesh of the separator mathematical model, additional horizontal sections were adopted every 0.5 cm at the horizontal walls of the working chambers and 1 or 2 horizontal to generate the gap cells (S4 c4 or S4 c6 mesh Fig. 12).

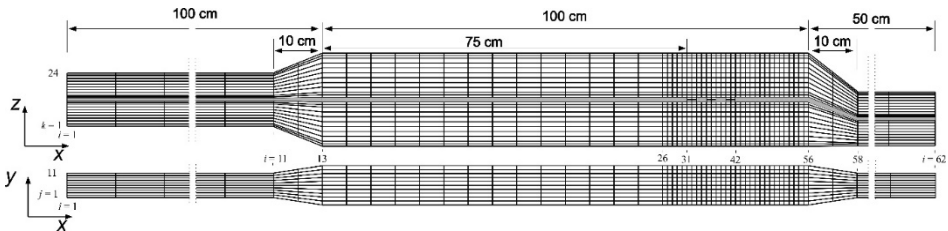


**Fig. 12.** Mathematical model mesh version S4c4

In the inlet section, the flow velocity was equal to the average velocity ( $Q/A$ ) in all cells. In subsequent sections (10 sections per 100 cm section) the water velocity in the cell was calculated, taking into account the roughness of the surface and the effect of cells excluded from the water flow. Cross-section  $I = 11$  is located directly in front of the separator diffuser on the plane  $\Pi_{yz}$ . Fig. 13 compares the velocity distributions obtained from simulations with the S1 and S4 grids. In both cases, the velocity distributions were symmetrical:

- in the upper and lower working chamber of the separator,
- on the left and right side of the chamber relative to the vertical surface.

The vertical and horizontal expansion of the separator working chambers causes changes in velocity distribution in subsequent sections. Fig. 14 presents horizontal velocity profiles in the  $\Pi_{xz}$  plane in sections 12, 13 and 14.

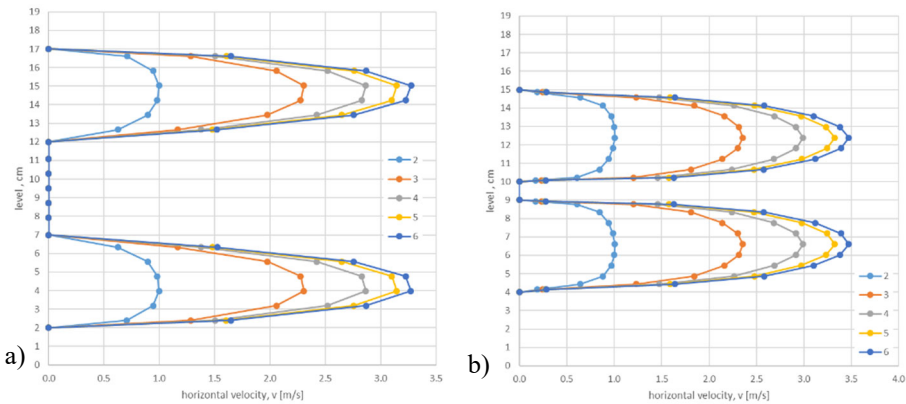


**Fig. 13.** Horizontal velocity distribution (projection onto the  $\Pi_{xz}$  plane) in selected section: a) mesh S1c2, b) mesh S3c4

The rapid extension of the cross-section in the original mesh version of the mathematical model (S1) causes a significant disturbance in the flow. There are opposite velocities directed at all the walls of the separator working chambers (left and right side, upper and lower surfaces of both working chambers). Such disturbances, especially in the lower part of the upper working chamber of the separator, cause the picking up of larger, dragged solid particles, which may reduce the efficiency of the separation process (Fig. 6). Changes to the separator design, including by gradual expansion it causes the area of disturbances and increased turbulence of the stream to be limited only to external areas (Fig. 7). The velocities at the bottom of the upper separator chamber (at the separation surface) will change slightly. As dragged, solid particles transported in the inlet pipe are still transported on the bottom.

During the simulation, the location of the first gap (as in the tests on the physical model) was assumed at the distance  $L_{1s} = 0.75L_k$  length of the working chamber. Analysis of velocity distribution in the case of a gentle extension (mesh S4 with diffuser) allows determining the minimum distance of the location of the first slot  $L_{1s}$  in half the length of the separator chamber  $L_k$ .

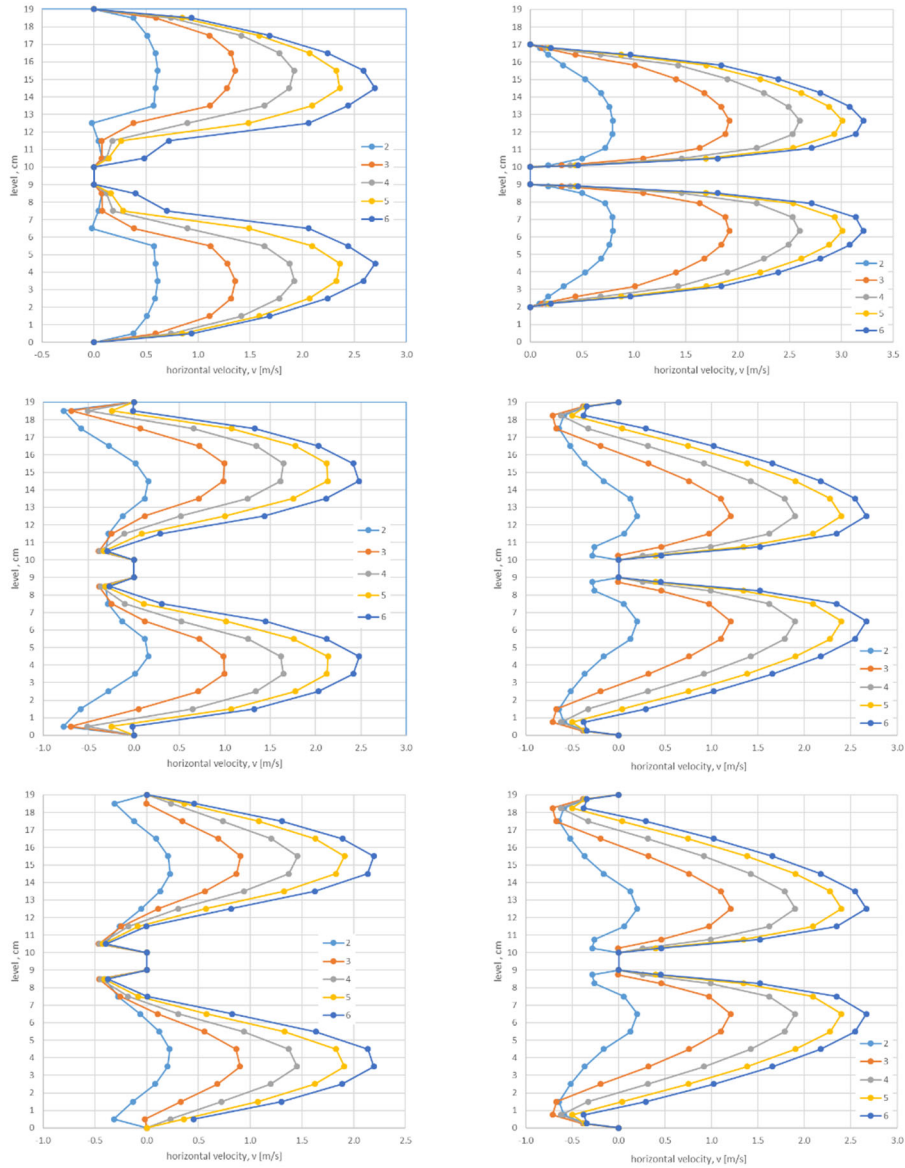


**Fig. 14.** Velocity distribution in the  $\Pi_{xz}$  plane in sections 12, 13 and 14: on the left is the S1c2 mesh; on the right, the S4c4 mesh

A comparison of velocity distributions directly through the first slot (cross-section 30) was shown in Fig. 15. Changing the geometry of the outlet section increased the velocity around the slots, allowing for the effective separation of selected sediment fractions.

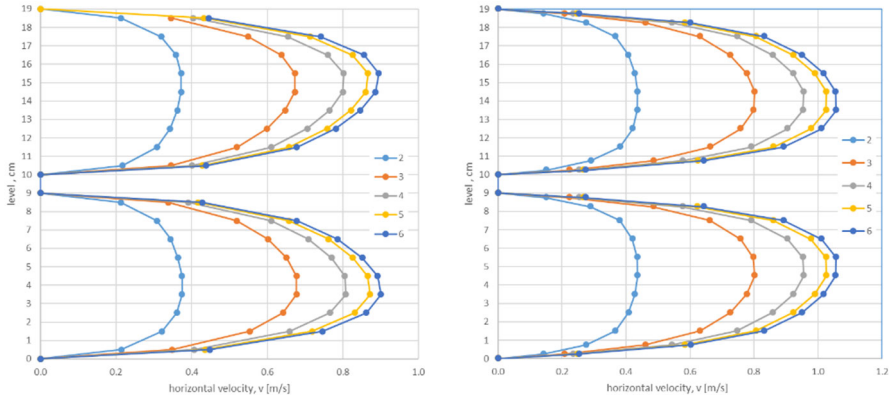


**Fig. 15.** Horizontal velocity distribution in vertical section 30: a) mesh S1c2, b) mesh S4c4

### 3. Summary

The sediment transport issues and its intensity variability during floods are an essential element of river network modelling, especially if flow continuity is interrupted by various hydrotechnical constructions. Bedload and suspension sediment can significantly cause silting up of the reservoir due to sedimentation processes, particularly intensified near dams, where the natural flow is interrupted. Therefore, ensuring the continuity of sediment flow through the river reservoir seems to be the right approach. A modified slotted separator has been proposed as an installation which allows the transport of sediments with simultaneously sorting them into two streams: thicker mineral particles directed directly to the river and fine mineral and organic fractions that can be utilised (forestry or agricultural use).

Developing an optimal separator design required many analyses and tests, both laboratory and numerical simulations. The construction of the separator was analysed in detail, including the geometry and arrangement of the separator inlet and outlet ducts, as well as the location of the gaps. The optimal solutions turned out to be the use of a diffuser on the inlet channels and the appropriate design of the outlet channels, including connection of the bottom of the pipe and the chamber on one level with simultaneous lowering of the discharge pipes and a mild narrowing of the cross-section through the introduction of a 10 cm

long confusor. Simulations also enabled the determination of the optimal position of the first slot sections at a distance  $L_{1s}$  equal to half the length of the separator chamber  $L_k$ .

The proposed modifications consider the reduction of turbulence in the flow, ensuring the continuity of water and sediment flow with simultaneous separation.

## References

- Abouzeid, G., Mohamed H.I., Ali S.M. (2007). 3-D numerical simulation of flow and clear water scour by interaction between bridge piers. *J. of Eng. Sciences*, Assiut University, Egypt, 35(4), 891-907.
- Agrawal, A.K. (2005). *Numerical Modelling of Sediment Flow in Tala Desilting Chamber*. M. Sc. Thesis, Department of Hydraulic and Environmental Engineering, Norwegian University of Science and Technology, Trondheim, Norway.
- Błoński, S. (2009). *Analiza przepływu turbulenty w mikrokanale*. Rozprawa doktorska, Zakład Mechaniki i Fizyki Płynów, Instytut Podstawowych Problemów Techniki Polskiej Akademii Nauk, Warszawa, Poland.
- Brandt, S.A. (1999). Reservoir Desiltation by Means of Hydraulic Flushing: Sedimentological and Geomorphological Effects in Reservoirs and Downstream Reaches As Illustrated by the Cachí Reservoir and the Reventazón River, Costa Rica. *Ph.D. thesis submitted to the Institute of Geography*, Faculty of Science, University of Copenhagen. *Geographica Hafniensia*, A8.
- Hämmerling, M., Błażejowski, R., Walczak, N. (2013). Modeling of local scour in non-cohesive soils below sills using SSIIM computer code. *Rocznik Ochrona Środowiska*, 15, 901-913.
- Hilldebrant, G., Klassen, I., Olsen, N.R.B (2017). 3D CFD modelling of velocities and sediment transport in the Iffezhiem hydropower reservoir. *Hydrology Research*, 48(1). 147-159. DOI: 10.2166/nh.2016.197
- Lauder, B.E., Spalding, D.B. (1974). The numerical computation of turbulent flows. *Computer Methods in Applied Mechanics and Engineering*, 3(2): 269-289.
- Madeyski, M., Michalec, B., Tarnawski, M. (2008): Zamulanie małych zbiorników wodnych i jakość osadów dennych. *Infrastruktura i Ekologia Terenów Wiejskich. 11*, Komisja Technicznej Infrastruktury Wsi PAN w Krakowie.
- Nieć, J., Zawadzki, P., Nowacki, F. (2019). Small Dam Drainage with Nonwoven Geotextile after 40 Years of Exploitation. *Appl. Sci.*, 9(19), 4161, DOI: 10.3390/app9194161
- Olsen, N.R.B. (2007). *Numerical Modelling and Hydraulics*. The Norwegian University of Science and Technology. Available on: <https://www.ntnu.edu/ivm/cfd>, September 2015.
- Olsen, N.R.B. (2009). *A three dimensional numerical model for simulation of sediments movements in water intakes with multiblock options*. The Norwegian University of Science and Technology, Available on: <https://www.ntnu.edu/ivm/cfd>, September 2015.

- Olsen, N.R.B. (2014). *A three-dimensional numerical model for simulation of sediment movements in water intakes with multiblock option. User's manual*. The Norwegian University of Science and Technology. Available on: <https://www.ntnu.edu/ivm/cfd>, September 2015.
- Parzonka, W., Kasperek, R., Głowski, R. (2010). Ocena degradacji koryta właściwego Odry środkowej i program działań naprawczych. *Infrastruktura i ekologia terenów wiejskich*, 8(1). PAN, Kraków, Poland. 59-68.
- Rodi, W. (1980). *Turbulence Models and their Application in Hydraulics, A State of the Art Review*. IAHR, Delft, Holandia.
- Rüther, N. (2006). *Computational fluid dynamics in fluvial sedimentation engineering*. Ph. D. Thesis, Department of Hydraulic and Environmental Engineering, Norwegian University of Science and Technology, Trondheim, Norway.
- Singh, T.P., Chandrashekar, J., Agrawal, A.K. (2007). *Analysis of water and sediment flow in desilting basin of a run-of-river hydroelectric project*. International Conference on Small Hydropower – Hydro Sri Lanka.
- Zawadzki, P., Błażejowski, R. (2018). Urządzenie do hydromechanicznego oczyszczania i usuwania osadów dennych ze zbiorników zaporowych. Patent 228599. *Wiadomości Urzędu Patentowego*, 4, Urząd Patentowy Rzeczypospolitej Polskiej, Warszawa, 208.
- Zawadzki, P., Kujawiak, S., Walczak, N., Oliskiewicz-Krzywicka, A. (2018): Investigation of a Slotted Separator for Hydromechanical Installation of Sludge Removal from a Water Reservoir. *Rocznik Ochrona Środowiska*, 20, 464-480.
- Zhang, Q., Hillebrand, G., Klassen, I., Vollmer, S., Olsen, N.R.B., Moser, H., Hinkelmann, R. (2013). *Sensitivity analysis of flow field simulation in the Iffezheim Reservoir in Germany with the 3D SSIIM model*. Proceedings of 2013 IAHR World Congress.
- Zhang, Q., Speckter, T., Hinkelmann, R., Hillebrand, G., Hoffmann, T., Moser, H. (2016). *Sensitivity of deposition and erosion to bed composition in the Iffezheim reservoir, Germany*. In: *River Sedimentation*, Taylor & Francis Group. DOI: 10.1201/9781315623207-146